Journal of Materials Chemistry

Cite this: *J. Mater. Chem.*, 2012, **22**, 11290

www.rsc.org/materials

PAPER

Functionalization of carbon and gold nanomaterials using PNIPAAm grafted dextran: a general route towards robust and smart nanomaterials†

Weipeng Lv,‡ Junjie Qi,‡ Wenqian Feng, Guoliang Zhang, Fengbao Zhang and Xiaobin Fan*

Received 8th February 2012, Accepted 28th March 2012
DOI: 10.1039/c2jm30753g

A universal functionalization platform based on PNIPAAm grafted dextran smart polymers for, but not limited to, carbon and gold nanomaterials, is developed. The dextran based smart polymer contains three indispensable components: 1) dextran – to provide hydrophilicity and stability; 2) PNIPAAm – to provide stimuli-sensitivity; 3) dodecylthiocarbonothioylthio groups (or aminolysis-generated thiols) – to provide feasible functionalization through stable interactions between polymer and nanomaterials. The readily accessible distinctive versions of polymers can provide necessary and efficient interactions with a variety of nanomaterials: the unique dodecyl end groups provide the effective functionalization of SWNT and NGO in a noncovalent manner, while the AuNR can be covalently functionalized through aminolysis-generated thiols. These functionalized nanomaterials are simultaneously endowed with well-retained properties of interest, excellent stability and smart properties: they exhibit superior stability under various conditions and the absorption, fluorescent and aggregation properties can be smartly tuned by temperature and NIR light. The establishment of this general approach is an important step forward for development and wide-application of smart nanomaterials in catalysts, actuators, sensors and biomedicine.

1. Introduction

As we have been seeing, carbon and gold nanomaterials have come up to the center of intensive research owing to their unique optical and electronic properties.[1] They have enabled tremendous progress in a wide range of areas including catalysis, biology, medicine, electronics, and sensors, among others.[2] Since most inorganic nanomaterials are insoluble or have a pronounced tendency to aggregate in water, appropriate functionalization is essential to endow them with sufficient aqueous stability while maintaining their intrinsic size- and shape-dependent properties for practical applications.[3] Despite progress in functionalization of nanomaterials using small molecule or polymer coatings to maintain stability, novel versatile nanomaterials and related applications have been pursued by incorporating existing nanomaterials with multifunctional polymers that not only retain their properties of interest, but also give access to novel fascinating structures and properties.[3c,4] As a specific example, smart nanomaterials that can dynamically and reversibly change their critical properties in response to external stimulus or environment have shown great potential in many biomedical and technical applications.[5] Smart polymer coatings can prevent nanomaterials from aggregation and additionally impart dynamically switchable properties to them, resulting in actual active systems. In this regard, much effort has been made to prepare smart nanomaterials through *in situ* formation or post covalent/noncovalent modification of nanomaterials, yet with few exceptions, each of these existing specific approaches is likely limited to produce only one or a few smart nanomaterials.[4d,6] The instability of these nanomaterials against harsh conditions has become one of the central obstacles for extensive applications. It is thus desired to develop a facile, efficient and general route to produce smart nanomaterials with superior stability under various conditions.

To meet these challenges, we herein aim to develop a multifunctional coating material that can simultaneously provide smart properties and excellent stability to a variety of nanomaterials through stable noncovalent/covalent functionalization. Dextran-based smart polymer, poly(*N*-isopropylacrylamide) (PNIPAAM) grafted dextran (DexPNI), which pivots around dodecylthiocarbonothioylthio groups linked to dextran, has been synthesized by reversible addition-fragmentation chain transfer (RAFT) polymerization of NIPAAm.[7] Dextran, a natural analogue of PEG (polyethylene glycol), is employed as the backbone of the smart polymers not only because of its excellent hydrophilicity, biocompatibility, biodegradability, but also due to its unique hyperbranched structure to provide a resistant coating for harsh conditions, as well as the reactive hydroxyl

School of Chemical Engineering and Technology, Tianjin University, Tianjin 300072, P.R. China. E-mail: xiaobinfan@tju.edu.cn

† Electronic supplementary information (ESI) available. See DOI: 10.1039/c2jm30753g

‡ These authors contributed equally.

groups for further chemical/biological modification.[3a,8] Since dextran itself cannot be tightly attached on the surface of nanomaterials,[3a] the dodecylthiocarbonothioylthio group introduced by esterification of dextran with 2-(dodecylthiocarbonothioylthio)-2-methyl-propanoic acid (DTM) serves as an essential component to provide steady bonding with carbon nanomaterials (by hydrophobic interactions) and gold nanomaterials (by aminolysis-generated thiol groups). The readily accessible distinctive versions of polymers, to provide necessary and efficient interactions with a variety of nanomaterials, are essential because the establishment of a general functionalization route only becomes feasible if the polymer can be tightly attached on the surface of nanomaterials. Meanwhile, this dextran derivates (DexDTM) is used as a macro chain transfer agent for the RAFT polymerization of PNIPAAm, which is a representative temperature-sensitive polymer exhibiting a lower critical transition temperature (LCST) above which the polymer becomes hydrophobic. To demonstrate the functionality of DexPNI, which has 12–13 DTM groups in one dextran chain and 48 NIPAAm units in one PNIPAAm chain, we use it to functionalize a series of carbon and gold nanomaterials that have strong absorption in the near-infrared (NIR) region for photothermal effect,[1f] including single-walled carbon nanotubes (SWNT),[2a,9] nanosized graphene oxide (NGO)[2e,10] and gold nanorods (AuNR).[2k,11] NIR light that deeply penetrates through tissues with low absorption can serve as a complementary stimulus of temperature where temperature changes may not be implemented.[4d,5a] When exposing to an NIR laser beam, these nanomaterials can absorb and convert light into heat by transferring electronic excitations into molecular vibration energies.[1f] The heat-induced elevation of local environment temperature will cause the LCST phase transition of PNIPAAm, and in turn result in the variation of the intrinsic properties of nanomaterials.[4d] Therefore, DexPNI functionalization provides a general and facile route to obtain a series of robust and smart nanomaterials that dually respond to temperature and NIR light.

2. Results and discussion

2.1. Functionalization of single-walled carbon nanotubes through noncovalent interactions

Single-walled carbon nanotubes (SWNT) are "rolled-up" cylindrical tubes of seamless single-layer graphene sheets, possessing sharp densities of electronic states at the van Hove singularities which result in unique optical properties, such as NIR absorption features, photoluminescence, and Raman scattering.[1a,9a,9b] SWNT is an especially challenging material to suspend and it is even more challenging to suspend SWNT by smart polymers without perturbing their critical physical spectroscopy properties. A central obstacle for their practical applications, especially in optics and biomedicine, is the perturbation of the electronic structure and related properties by bundling of the tubes due to strong van der Waals binding energy of tube–tube contact. To this end, it is essential to nonperturbingly coat SWNT with amphiphilic surfactant molecules or polymers only *via* a noncovalent approach.[1a,2a,3a,12] Although various amphiphiles have been employed to bind with SWNT through π–π stacking, van der Waals forces and hydrophobic interactions to obtain aqueous SWNT suspension, it is still challenging to maintain the properties of interest under harsh conditions especially by using smart polymers that are able to tune the intrinsic properties of SWNT by external stimuli.[3a,6a–c] In our case, raw HiPco SWNT powder can be well suspended in DexPNI solution (5 mg ml^{-1}) after tip-sonication for 30 min with 450 W power level and subsequent centrifuge-removal of unsuspended impurities at 23 000 g for 4 h. As shown in Fig. 1b, the UV-vis-NIR spectra of DexPNI-suspended SWNT attest the representative van Hove singularities of well-dispersed HiPco SWNT with sharp interband E_{11} and E_{22} transitions.[1a] Raman spectra in Fig. S1 show that the tangential mode (G-band) of DexPNI–SWNT upshifts by 7 cm^{-1}, probably due to the compressive strain induced by DexPNI functionalization.† Since covalent modification of SWNT causes significant changes in nanotubes bonds which will result in the increase in the intensity of disorder-induced mode (D-band) and disappearance of the van Hove singularities in the UV-vis-NIR spectum,[13] the low intensity of D-band of DexPNI–SWNT confirms that DexPNI and SWNT are noncovalently interacted with each other. Moreover, these aqueous suspensions exhibit remarkable long-term stability at extreme pH and high salt concentration without any macroscopic aggregation or significant changes in UV-vis-NIR absorption spectra. Although the DexPNI–SWNT composite cannot be directly redispersed in water after freeze-drying, it still can be stored in powder form since the stable DexPNI–SWNT suspension, which has the same UV-vis-NIR absorption spectra as before freeze-drying, can be simply recovered by 2 min sonication or 1 h gentle stirring. This result is important because most SWNT suspended by smart polymers exhibit broader van Hove transitions, precipitate under extreme pH, high salt concentration and high speed

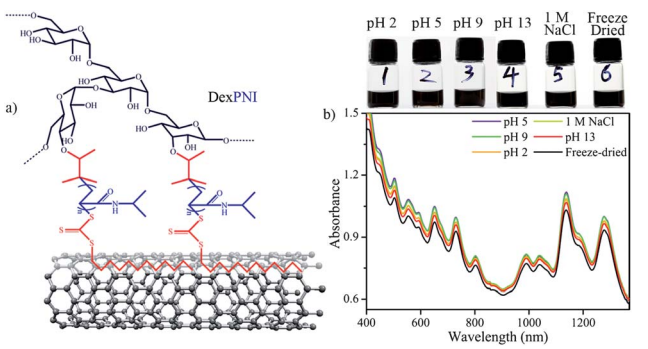

Fig. 1 SWNT functionalized by dextran-based smart polymer. a) Schematic illustration of SWNT functionalization using PNIPAAm grafted dextran with dodecyl end groups (DexPNI). DexPNI are tightly anchored on SWNT surfaces by noncovalent interactions between dodecyl groups and SWNT. b) Pictures (top panel) and UV-vis-NIR spectra of DexPNI functionalized SWNT at various conditions. The wavelength ranges of lowest energy semiconducting, second lowest semiconducting, and lowest metallic absorption peaks are 900–1400 nm, 600–900 nm and 400–600 nm, respectively. The excellent stability of DexPNI–SWNT is demonstrated by the well maintained black color and characteristic UV-vis-NIR peaks after incubation at extreme pH (ranging from 2 to 13 for 4 weeks) and high salt concentration (1 M NaCl for one week), as well as after sonication-assisted redispersion of freeze-dried sample. See also Fig. S2 for stability tests of SWNT functionalized by non-smart dextran-based macro chain transfer agent (DexDTM) against harsh conditions including heating.†

centrifugation, and cannot be simply resuspended in water after freeze-drying.[6a,9c,14] Therefore, DexPNI can be tightly attached on SWNT in water through hydrophobic (noncovalent) interactions between dodecyl end groups and SWNT, yielding robust, smart and well-suspended SWNT aqueous solutions.

When the PNIPAAm side chains of DexPNI, which are strongly interacted with the side walls of SWNT, undergo a phase transition from hydrophilic to hydrophobic state above LCST,[15] DexPNI–SWNT become hydrophobic and are likely to form large self aggregates through "increased" hydrophobic interactions and side-by-side contact between SWNT. Thus, the dispersion/aggregation states of DexPNI–SWNT will be significantly affected by temperature/NIR irradiation and cause corresponding changes in the spectroscopy properties. Given the above assumptions, UV-vis and fluorescence spectra of DexPNI–SWNT at different temperatures or upon 808 nm NIR laser irradiation (power density = 1.5 W cm^{-2}) are shown in Fig. 2. At 25 °C (below LCST), DexPNI on SWNT is hydrophilic and in extended state, resulting in the well-suspended DexPNI–SWNT solutions with representative UV-vis and fluorescence spectra. When the temperature is increased above LCST or upon NIR irradiation, we can observe: 1) significant increase in UV-vis absorbance mostly due to the phase transition of PNIPAAm;[15] 2) blue-shift and broadening of absorption peaks induced by SWNT aggregation; 3) partial quenching of fluorescence which also indicates the aggregation of SWNT; and 4) turbid solution with macroscopic precipitate of SWNT. Particularly, the NIR-response of DexPNI–SWNT is very fast since the solution starts to become turbid immediately from the spot exposed to NIR laser and then the whole solution becomes turbid gradually, accompanying with the emerging of SWNT precipitates. Although the spectroscopy properties and aggregation state cannot be directly recovered by cooling back to 25 °C, it is still worth noting that, by 2 min sonication, the heated solution can be well redispersed and has nearly the same spectroscopy properties as original suspension. The reversible control of SWNT aggregations using external stimuli meets the potential application demands in SWNT-based switching devices, catalysis, sensors, and especially in biological field.[14b,16]

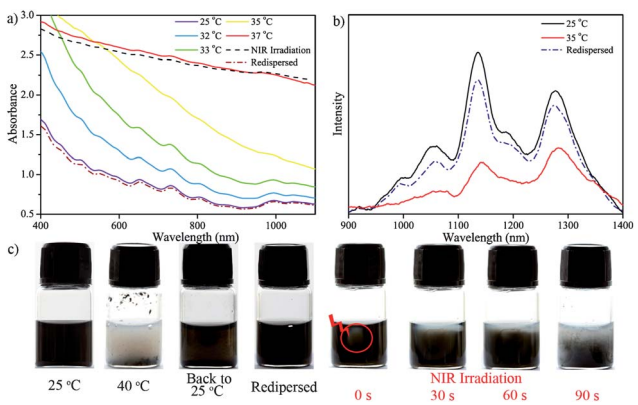

Fig. 2 Temperature/NIR sensitivity of DexPNI–SWNT. a) UV-vis spectra of DexPNI–SWNT below and above LCST (~32 °C), upon NIR irradiation, and after redispersion of heated sample by 2 min sonication at 25 °C. b) Fluorescence emission spectra (λ_{exc} = 410 nm) of DexPNI–SWNT before and after heating to 35 °C, and after sonication-assisted redispersion of heated sample. No fluorescence could be detected at 40 °C when LCST phase transition of DexPNI and macroscopic precipitation of SWNT are completed. c) From left to right: pictures of DexPNI–SWNT suspension at 25 °C, 40 °C (neither shaking nor sonication can prevent SWNT precipitation), after cooling back to 25 °C (some of SWNT remain as precipitates), after redispersion by 2 min sonication at 25 °C (precipitates are fully resuspended), and upon 808 nm NIR laser irradiation (power density = 1.5 W cm^{-2}, phase transition starts immediately at NIR exposure spot and gradually spreads to the whole suspension). See also Fig. S8 for temperature evolution curves for these NIR-sensitive solution upon laser irradiation.†

2.2. Functionalization of nano-graphene oxide through noncovalent interactions

Graphene—a flat monolayer of carbon atoms tightly packed into a two-dimensional honeycomb lattice—has become a rising star in the materials research community after its discovery in 2004[17] and potential biomedical applications of graphene have been pursued by various groups since 2008.[2e,10b,18] In contrast to graphene with a zero band gap, graphene oxide (GO) possessing intrinsic fluorescence in UV to NIR ranges and exceptional fluorescence-quenching ability is especially attractive for optical sensing and imaging applications.[10a,19] Although GO is soluble in water, its aqueous stability still needs to be enhanced against harsh conditions for more widely applications.[18b,20] Having proved the excellent performance of DexPNI to functionalize one-dimensional carbon allotropes (SWNT), we next devote to preparing a robust and smart two-dimensional carbon nanomaterial based on nanosized graphene oxide (NGO) and DexPNI. Tip-sonication at 450 W power level for 90 min is employed to break GO (obtained from graphite oxide by Hummers method[21]) into NGO with 50–120 nm in size; see Fig. S3 for AFM image of NGO.† To avoid the further sonication breaking of NGO, DexPNI–NGO solution is obtained by overnight-stirring of DexPNI (5 mg ml^{-1}) and NGO (0.5 mg ml^{-1}) mixture. In the Raman spectrum of DexPNI–NGO (Fig. S4†), the D-band at around 1329 cm^{-1} corresponds to defects in the curved NGO sheet, and staging disorder, while the G-band at 1593 cm^{-1} is related to the graphitic hexagon-pinch mode.[22] After DexPNI functionalization, the I_D/I_G intensity ratio has no obvious change while G-band upshifts by 7 cm^{-1}, indicating that the functionalization process is noncovalent and does not reduce the size of in-plane sp^2 domains. Similar with DexPNI–SWNT, DexPNI–NGO suspensions also show excellent long-term stability at extreme pH (ranging from 2 to 13 for 4 weeks) and high salt concentration (1 M NaCl for one week) without obvious change in NGO dispersity or UV-vis absorption spectra; see Fig. S5 and S6.† Since NGO is more hydrophilic than SWNT, DexPNI–NGO can be readily redispersed in water after freeze-drying just by gentle shaking rather than sonication, providing the opportunity to produce redispersible smart NGO in powder form. However, it should be noted that the hydrophilic nature of NGO does not always lead to good redispersion after freeze-drying.

In regard of temperature/NIR sensitivity, UV-vis spectra show that the absorbance of DexPNI–NGO greatly increases upon heating or NIR irradiation (Fig. 3c). This turbidity change is mainly induced by the LCST phase transition of PNIPAAm. The absorbance peak at 209 nm, which corresponds to a π-electron

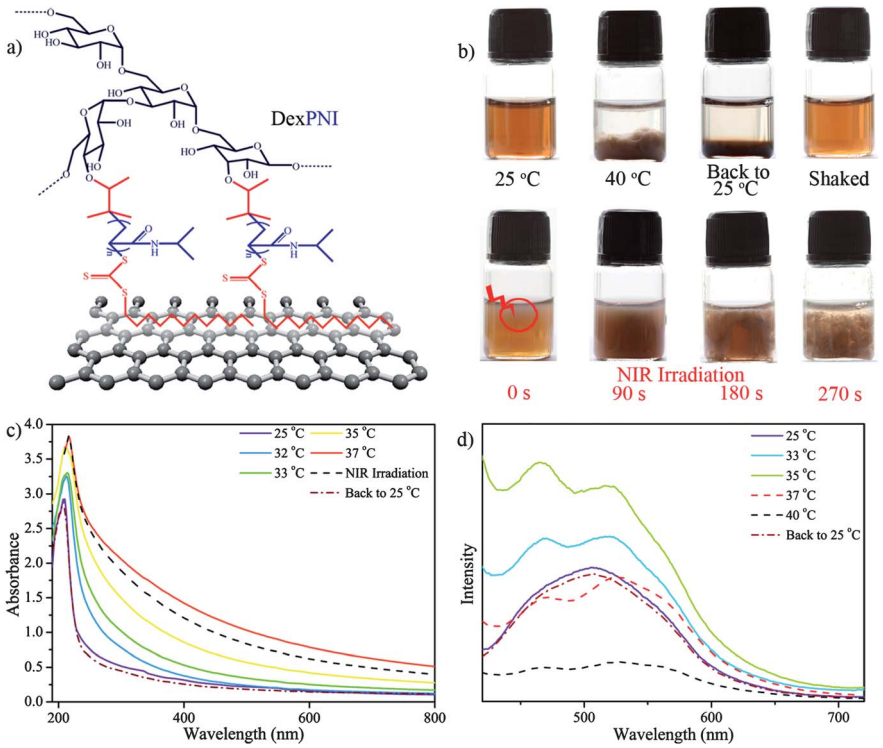

Fig. 3 NGO functionalized by dextran-based smart polymer. a) Schematic illustration of NGO functionalization using DexPNI, which are tightly anchored on NGO by noncovalent interactions between dodecyl groups and NGO. b) Pictures of DexPNI–NGO suspension at 25 °C, 40 °C (neither shaking nor sonication can prevent NGO precipitation, the upper solution is clear instead of cloudy), after cooling back to 25 °C (most NGO remain as precipitates), after redispersion by gentle shaking at 25 °C (precipitates are readily and fully resuspended), and upon NIR irradiation (phase transition starts immediately at NIR exposure spot and gradually spreads to the whole suspension, accompanying with NGO aggregation). c) UV-vis spectra of DexPNI–NGO below and above LCST (~32 °C), upon NIR irradiation, and after shaking-assisted redispersion of heated sample at 25 °C. d) Fluorescence emission spectra ($\lambda_{exc} = 380$ nm) of DexPNI–NGO upon heating, and after shaking-assisted redispersion of heated sample at 25 °C. Two-stage variation in fluorescence intensity is observed: increase at 25 to 35 °C (solid lines) when PNIPAAm chains are not fully dehydrated; and decrease at 35 to 40 °C (dash lines) when LCST phase transition of DexPNI and macroscopic precipitation of NGO are completed.

plasmon excitation of graphitic carbon,[22a] red-shifts to 216 nm when the temperature is increased from 25 °C to 40 °C or after NIR irradiation. A similar red-shift has been observed with the increase of NGO size or reduction degree.[22a,23] As shown in Fig. 3b, when NGO is totally precipitated at 40 °C, the solution becomes nearly transparent, leaving little free polymer in the solution phase, while the DexPNI–SWNT solution remains opaque during precipitation. The difference in turbidity of heated solution implies that DexPNI is tightly anchored on NGO surfaces and has stronger interactions with NGO than SWNT. Serendipitously, heating DexPNI–NGO solution from 25 to 35 °C results in great enhancement of fluorescence intensity with the emerging of dual-peak fluorescence at 468 and 523 nm from a single peak at 507 nm (Fig. 3d). In this temperature range, the phase transition of DexPNI is incomplete and no macroscopic precipitation of NGO can be observed. On the contrary, further increasing of temperature to 40 °C led to significantly damped fluorescence intensity. The temperature-induced variation in absorption and fluorescence peak position and increase in fluorescence intensity are not yet fully understood but may be ascribed to the LCST phase transition induced change of refractive index and dielectric constant of surrounding medium.[10a,18b] The partial quenching of fluorescence at temperature higher than 35 °C is due to the precipitation of NGO when PNIPAAm chains are completely dehydrated. When heated NGO suspension is cooled back to 25 °C the dispersity and UV-vis absorbance can be recovered to the original level by gentle shaking, which is suggestive of the readily reversible nature of temperature/NIR regulated aggregation behaviors of DexPNI–NGO. Since we and other groups have shown promising catalysis applications of graphene/GO (derivates) and their nanometal composites,[24] besides the potential applications in optics and biology, this readily-accessible smart aggregation property may be used to build recyclable catalytic systems that can be reversibly switched on and off *via* remote triggered aggregation of catalyst.[25]

2.3. Functionalization of gold nanorods through covalent interactions

Gold nanorods (AuNR) that exhibit size- and shape-tunable surface plasmon resonance from visible to NIR regions are of particular interest in bioimaging, biosensing and biomedicine.[2k,11b] In addition to functionalize carbon nanomaterials in a noncovalent manner, our smart polymer can be covalently anchored onto the surface of gold nanomaterials through a gold–thiol linkage. This can be achieved by aminolysis of DexPNI to convert trithiocarbonate groups into thiol groups under

anaerobic condition at 5–10 °C. Cylindrical AuNR prepared by seed-mediated growth method is gold nanorods (AuNR) that exhibit size- and shape-tunable surface plasmon resonance from visible to NIR regions are of particular interest in bioimaging, biosensing and biomedicine.[2k,11b] Cylindrical AuNR prepared by seed-mediated growth method is stepwise washed twice by centrifuge, sonicated together with thiol-terminated DexPNI (SH-DexPNI) and dialyzed against water to fully replace CTAB surfactant with SH-DexPNI. The surface coating replacement results in a slight red shift in longitudinal plasmon peak at 760 nm because of the change in the dielectric environment of AuNR.[1f,3a,26] After functionalization, these AuNR show superior stability under various conditions. As shown in Fig. S7, neither precipitation nor obvious change of absorption spectra is observed after incubation in a wide range of pH of 2 to 13 (for 4 weeks) or 1 M NaCl solutions (for 1 week).† After redispersion of freeze-dried AuNR in water, they display almost the same absorption spectrum as before freeze-drying. Moreover, AuNR solution remains suspended upon heating at 80 °C for 6 h and regains the UV-vis absorbance when cooling back to room temperature. The temperature/NIR sensitivity of SH-DexPNI–AuNR is illustrated by the fact that, upon increasing of temperature to 40 °C or NIR irradiation, the surface plasmon band of AuNR red-shifts by 21 nm and becomes boarder (Fig. 4b). Also, the increase in turbidity and optical absorbance can be observed accompanying with the color change of solution from transparent light-brown to opaque dark-brown. Comparing with DexPNI–SWNT and DexPNI–NGO, this opaque solution does not precipitate while the aggregation of AuNR indeed occurs, as indicated by the rise of a shoulder peak at around 950 nm. The origin of this temperature-tunable optical property of AuNR is the LCST phase transition of PNIPAAm chains anchored on AuNR surfaces. Above LCST, the heat-induced intrachain collapse of PNIPAAm results in the formation of hydrophobic surface on AuNR, which further develops into a macroscopic coacervate phase.[27] As a consequence, the local dielectric constant and refractive index of the solution are changed with a concomitant aggregation of AuNR, thus altering the optical properties of AuNR.[26–28] The heat-induced variation in AuNR optical properties is also reversible as the UV-vis absorbance gets recovered upon cooling back to 25 °C.

3. Conclusions

In summary, we have demonstrated a universal functionalization platform based on PNIPAAm grafted dextran smart polymers for, but are not limited to, carbon and gold nanomaterials. The unique dodecyl end groups provide the effective functionalization of SWNT and NGO in a noncovalent manner, while the AuNR can be covalently functionalized through aminolysis-generated thiols. These functionalized nanomaterials are simultaneously endowed with well-retained properties of interest, excellent stability and smart properties: they exhibit superior stability under various conditions and the absorption, fluorescent and aggregation properties can be smartly tuned by temperature and NIR light. By using monomers other than NIPAAM, the present approach can be further used to build a vast variety of robust and multi-responsive nanomaterials. The establishment of this general approach is an important step forward for development and wide-application of smart nanomaterials in catalysts, actuators, sensors and biomedicine.

4. Experimental section

Reagents and materials

Dextran ($M_n \approx 70\,000$, Seebio Biotechnology), 2,2′-azobis[2-(2-imidazolin-2-yl)propane] (VA-044, Wako), raw HiPco single-walled carbon nanotubes (SWNT, Unidym, >65% carbon) and isopropylamine (IPA, Aldrich) were used as received. *N*-Isopropylacrylamide (NIPAAm, Aldrich) was purified by recrystallization from hexane. 2-(Dodecylthiocarbonothioylthio)-2-methylpropanoic acid (DTM) was synthesized according to the

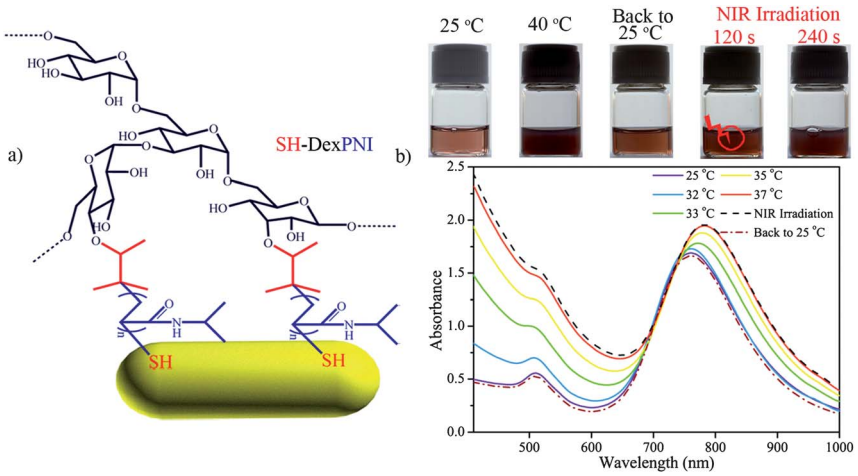

Fig. 4 AuNR functionalized by dextran-based smart polymer. a) Schematic illustration of AuNR functionalization using SH-DexPNI, which is generated by aminolysis of DexPNI. SH-DexPNI is tightly anchored on AuNR by gold–thiol covalent interactions. b) Pictures (top panel) of SH-DexPNI–AuNR suspension at 25 °C, 40 °C (the solution remains cloudy dark-brown upon either shaking or sonication), after cooling back to 25 °C (the clear light-brown solution gets recovered), and upon NIR irradiation (phase transition and color change start immediately at NIR exposure spot and gradually spreads to the whole suspension); UV-vis spectra of functionalized AuNR below and above LCST (~32 °C), upon NIR irradiation, and after cooling back to 25 °C.

literature.[29] All other reagents were purchased from commercial sources and used as received.

Synthesis of PNIPAAm grafted dextran with dodecyl end groups (DexPNI)

DexPNI was synthesized by a RAFT polymerization process as our previous reports.[7a,7c] In brief, the macro chain transfer agent (DexDTM) was first synthesized by esterification of 2-(dodecylthiocarbonothioylthio)-2-methylpropanoic acid chloride with hydroxyl groups of dextran using 4-dimethylaminopyridine and triethylamine as esterification catalyst. The number of dodecyl groups linked to dextran can be controlled by feed ratio of DTM to dextran. The DexDTM we used in this work contains 12–13 dodecyl end groups in one dextran chain as determined by ^{1}H NMR.[7c] The initial ratio of NIPAAm to DexDTM can also be used to adjust the average number of monomer per grafted PNIPAM chain. To ensure the fast and sharp phase transition of DexPNI, appropriate chain length is needed. According to our previous research on chain length dependent phase transition of DexPNI, the average PNIPAAm chain length of DexPNI we used here was 48 as estimated by ^{1}H NMR.[7a] In a typical synthesis procedure, NIPAAm (0.62 g, 5.5 mmol), water-soluble initiator VA-044 (0.18 g, 0.55 mmol) and DexDTM (0.6 g) were dissolved in water (120 mL) at 5–10 °C under a N_2 atmosphere and the solution was kept at 60 °C for 4 h. DexPNI was purified by dialysis against water and isolated by freeze-drying.

SWNT functionalization using DexPNI and DexDTM

10 ml solutions of DexPNI and DexDTM in deionized ultrafiltered water with the concentrations of 5 mg ml^{-1} and 2.5 mg ml^{-1} respectively were prepared and then centrifuged at 23 000 g for 15 min to remove the undissolved impurity. 2 mg of raw HiPco SWNT was added to the supernatant and then ultrasonicated for 30 min using a tip-sonicater at 450 W power. The solution temperature was kept below 25 °C using a circulator bath. Well suspended SWNT solutions were obtained after centrifugation at 23 000 g for 4 h to remove the unsuspended aggregates.

Synthesis of NGO and its functionalization using DexPNI and DexDTM

GO was prepared and purified according to the Hummers method.[21] An exfoliated suspension (5 ml, ~1 mg ml^{-1}) was obtained by dispersing purified GO in distilled water with the aid of intensive sonication for 1 h at 100 W power. This solution was first centrifuged at 2000 g for 15 min and then the supernatant was centrifuged at 23 000 g for another 15 min. After carefully removing the supernatant with a pipet, NGO with hundred-nanometer diameter was obtained by redispersion of GO with 5 ml water and subsequent ultrasonication at 450 W for 90 min. The solution temperature was kept below 25 °C using a circulator bath. 5 ml solutions of DexPNI and DexDTM in deionized ultrafiltered water with the concentrations of 10 mg ml^{-1} and 5 mg ml^{-1} respectively were prepared and then centrifuged at 23 000 g for 15 min to remove the undissolved impurity. The as prepared 5 ml DexPNI (or DexDTM) solution was mixed with 5 ml NGO solution and stirred overnight to obtain the functionalized NGO.

Synthesis of AuNR and its functionalization using SH-DexPNI

AuNR with controlled aspect ratio were synthesized using a typical seed-mediated, CTAB surfactant directed procedure by El-Sayed.[30] In order to convert the trithiocarbonate groups of DexPNI into thiol groups by aminolysis, 25 μl IPA was added to a 5 ml solution of N_2-bubbled DexPNI (5 mg ml^{-1}) under vigorous stirring.[7a,7c] The solution temperature was kept at 5–10 °C using an ice–water bath. The aminolysis reaction was allowed to proceed for 2 h under N_2 atmosphere, resulting in the thiol-terminated version of smart polymer (SH-DexPNI). To fully exchange CTAB with SH-DexPNI, 5 ml solution of as-prepared AuNR was first sonicated for 15 min to redissolve the precipitated CTAB and then washed twice by centrifugation at 23 000 g for 15 min while the supernatant was replaced with fresh water. This AuNR solution was mixed with the as-prepared SH-DexPNI and sonicated for 20 min. After dialysis against water for 3 days using a MWCO 14 000 dialysis tube, CTAB-free AuNR–SH-DexPNI suspension was obtained.

Characterization

^{1}H NMR spectra were obtained on a Bruker DRX-500 spectrometer operating at 500 MHz. Atomic force microscopy (AFM) was carried out on a CSPM 5000 scanning probe microscope in tapping mode. Raman spectroscopy was taken on an NT-MDT NTEGRA Spectra AFM-Raman system. The TEM image was taken on a Philips Tecnai G2 F20 high-resolution transmission electron microscopy. The optical properties of the DexPNI functionalized nanomaterials were characterized using a Unico 2802 UV-vis absorbance spectrometer, Shimadzu UV-3600 UV-vis-NIR absorbance spectrophotometer, Perkin-Elmer LS-55 fluorescence spectrophotometer (for NGO) and Jobin Yvon FL3-221-TCSPC fluorescence spectrophotometer (for SWNT). For UV-vis measurements, the temperature of the sample solutions was controlled within ±0.1 °C by circulating water baths linked to the equipment.

Acknowledgements

We thank Yang Li and Junyi Ji, Tianjin University, for synthesizing graphene oxide and Raman measurements. We also acknowledge the financial support from Doctoral Program of Higher Education (No. 20100032120017), Programme of Introducing Talents of Discipline to Universities (No. B06006), Tianjin Natural Science Foundation (No. 11JCYBJC01700), and Outstanding Ph.D. Thesis Foundation of Tianjin University.

References

1 (*a*) M. J. O'Connell, S. M. Bachilo, C. B. Huffman, V. C. Moore, M. S. Strano, E. H. Haroz, K. L. Rialon, P. J. Boul, W. H. Noon, C. Kittrell, J. Ma, R. H. Hauge, R. B. Weisman and R. E. Smalley, *Science*, 2002, **297**, 593–596; (*b*) H.-P. Boehm, *Angew. Chem., Int. Ed.*, 2010, **49**, 9332–9335; (*c*) A. K. Geim, *Angew. Chem., Int. Ed.*, 2011, **50**, 6966–6985; (*d*) K. S. Novoselov, *Angew. Chem., Int. Ed.*, 2011, **50**, 6986–7002; (*e*) M.-C. Daniel and D. Astruc, *Chem. Rev.*, 2004, **104**, 293–346; (*f*) X. M. Lu, M. Rycenga, S. E. Skrabalak, B. Wiley and Y. N. Xia, *Annu. Rev. Phys. Chem.*, 2009, **60**, 167–192.

2 (*a*) Z. Liu, S. Tabakman, K. Welsher and H. Dai, *Nano Res.*, 2009, **2**, 85–120; (*b*) W. Choi, S. Hong, J. T. Abrahamson, J.-H. Han, C. Song, N. Nair, S. Baik and M. S. Strano, *Nat. Mater.*, 2010, **9**, 423–429; (*c*) R. Bhowmick, S. Rajasekaran, D. Friebel, C. Beasley, L. Jiao, H. Ogasawara, H. Dai, B. Clemens and A. Nilsson, *J. Am. Chem. Soc.*, 2011, **133**, 5580–5586; (*d*) A. K. Geim, *Science*, 2009, **324**, 1530–1534; (*e*) Z. Liu, J. T. Robinson, S. M. Tabakman, K. Yang and H. Dai, *Mater. Today*, 2011, **14**, 316–323; (*f*) C. N. R. Rao, A. K. Sood, K. S. Subrahmanyam and A. Govindaraj, *Angew. Chem., Int. Ed.*, 2009, **48**, 7752–7777; (*g*) M. Liu, X. Yin, E. Ulin-Avila, B. Geng, T. Zentgraf, L. Ju, F. Wang and X. Zhang, *Nature*, 2011, **474**, 64–67; (*h*) M. Haruta, *Nature*, 2005, **437**, 1098–1099; (*i*) J. N. Anker, W. P. Hall, O. Lyandres, N. C. Shah, J. Zhao and R. P. Van Duyne, *Nat. Mater.*, 2008, **7**, 442–453; (*j*) David A. Giljohann, Dwight S. Seferos, Weston L. Daniel, Matthew D. Massich, Pinal C. Patel and Chad A. Mirkin, *Angew. Chem., Int. Ed.*, 2010, **49**, 3280–3294; (*k*) C. M. Cobley, J. Chen, E. C. Cho, L. V. Wang and Y. Xia, *Chem. Soc. Rev.*, 2011, **40**, 44–56.

3 (*a*) A. P. Goodwin, S. M. Tabakman, K. Welsher, S. P. Sherlock, G. Prencipe and H. Dai, *J. Am. Chem. Soc.*, 2009, **131**, 289–296; (*b*) D. Li, M. B. Muller, S. Gilje, R. B. Kaner and G. G. Wallace, *Nat. Nanotechnol.*, 2008, **3**, 101–105; (*c*) J. Shan and H. Tenhu, *Chem. Commun.*, 2007, 4580–4598; (*d*) A. S. Karakoti, S. Das, S. Thevuthasan and S. Seal, *Angew. Chem., Int. Ed.*, 2011, **50**, 1980–1994; (*e*) S. Wang, L. A. l. Tang, Q. Bao, M. Lin, S. Deng, B. M. Goh and K. P. Loh, *J. Am. Chem. Soc.*, 2009, **131**, 16832–16837.

4 (*a*) Z. Spitalsky, D. Tasis, K. Papagelis and C. Galiotis, *Prog. Polym. Sci.*, 2010, **35**, 357–401; (*b*) T. Ramanathan, A. A. Abdala, StankovichS, D. A. Dikin, M. Herrera Alonso, R. D. Piner, D. H. Adamson, H. C. Schniepp, ChenX, R. S. Ruoff, S. T. Nguyen, I. A. Aksay, R. K. Prud'Homme and L. C. Brinson, *Nat. Nanotechnol.*, 2008, **3**, 327–331; (*c*) J. R. Potts, D. R. Dreyer, C. W. Bielawski and R. S. Ruoff, *Polymer*, 2011, **52**, 5–25; (*d*) M. S. Yavuz, Y. Cheng, J. Chen, C. M. Cobley, Q. Zhang, M. Rycenga, J. Xie, C. Kim, K. H. Song, A. G. Schwartz, L. V. Wang and Y. Xia, *Nat. Mater.*, 2009, **8**, 935–939; (*e*) G. Prencipe, S. M. Tabakman, K. Welsher, Z. Liu, A. P. Goodwin, L. Zhang, J. Henry and H. Dai, *J. Am. Chem. Soc.*, 2009, **131**, 4783–4787.

5 (*a*) M. Yoshida and J. Lahann, *ACS Nano*, 2008, **2**, 1101–1107; (*b*) M. A. C. Stuart, W. T. S. Huck, J. Genzer, M. Muller, C. Ober, M. Stamm, G. B. Sukhorukov, I. Szleifer, V. V. Tsukruk, M. Urban, F. Winnik, S. Zauscher, I. Luzinov and S. Minko, *Nat. Mater.*, 2010, **9**, 101–113.

6 (*a*) D. Wang and L. W. Chen, *Nano Lett.*, 2007, **7**, 1480–1484; (*b*) J. C. Grunlan, L. Liu and Y. S. Kim, *Nano Lett.*, 2006, **6**, 911–915; (*c*) K. C. Etika, F. D. Jochum, P. Theato and J. C. Grunlan, *J. Am. Chem. Soc.*, 2009, **131**, 13598–13599; (*d*) Y. Shen, M. Kuang, Z. Shen, J. Nieberle, H. W. Duan and H. Frey, *Angew. Chem., Int. Ed.*, 2008, **47**, 2227–2230.

7 (*a*) W. Lv, S. Liu, W. Feng, J. Qi, G. Zhang, F. Zhang and X. Fan, *Macromol. Rapid Commun.*, 2011, **32**, 1101–1107; (*b*) W. Lv, Y. Wang, W. Feng, J. Qi, G. Zhang, F. Zhang and X. Fan, *J. Mater. Chem.*, 2011, **21**, 6173–6178; (*c*) W. Lv, S. Liu, X. Fan, S. Wang, G. Zhang and F. Zhang, *Macromol. Rapid Commun.*, 2010, **31**, 454–458.

8 (*a*) H. Jang, Y. K. Kim, S. R. Ryoo, M. H. Kim and D. H. Min, *Chem. Commun.*, 2010, **46**, 583–585; (*b*) S. R. Van Tomme and W. E. Hennink, *Expert Rev. Med. Devices*, 2007, **4**, 147–164.

9 (*a*) J. Robinson, K. Welsher, S. Tabakman, S. Sherlock, H. Wang, R. Luong and H. Dai, *Nano Res.*, 2010, 1–15; (*b*) K. Welsher, Z. Liu, S. P. Sherlock, J. T. Robinson, Z. Chen, D. Daranciang and H. Dai, *Nat. Nanotechnol.*, 2009, **4**, 773–780; (*c*) T. Fujigaya, T. Morimoto, Y. Niidome and N. Nakashima, *Adv. Mater.*, 2008, **20**, 3610–3614.

10 (*a*) K. P. Loh, Q. Bao, G. Eda and M. Chhowalla, *Nat. Chem.*, 2010, **2**, 1015–1024; (*b*) X. Sun, Z. Liu, K. Welsher, J. Robinson, A. Goodwin, S. Zaric and H. Dai, *Nano Res.*, 2008, **1**, 203–212; (*c*) K. Yang, S. Zhang, G. Zhang, X. Sun, S. T. Lee and Z. Liu, *Nano Lett.*, 2010, **10**, 3318–3323.

11 (*a*) E. C. Dreaden, M. A. Mackey, X. Huang, B. Kang and M. A. El-Sayed, *Chem. Soc. Rev.*, 2011, **40**, 3391–3404; (*b*) K.-W. Hu, T.-M. Liu, K.-Y. Chung, K.-S. Huang, C.-T. Hsieh, C.-K. Sun and C.-S. Yeh, *J. Am. Chem. Soc.*, 2009, **131**, 14186–14187.

12 N. Karousis, N. Tagmatarchis and D. Tasis, *Chem. Rev.*, 2010, **110**, 5366–5397.

13 (*a*) C. Menard-Moyon, N. Izard, E. Doris and C. Mioskowski, *J. Am. Chem. Soc.*, 2006, **128**, 6552–6553; (*b*) J. L. Hudson, M. J. Casavant and J. M. Tour, *J. Am. Chem. Soc.*, 2004, **126**, 11158–11159.

14 (*a*) Y. Z. You, C. Y. Hong and C. Y. Pan, *Adv. Funct. Mater.*, 2007, **17**, 2470–2477; (*b*) C.-Y. Hong and C.-Y. Pan, *J. Mater. Chem.*, 2008, **18**, 1831–1836.

15 H. G. Schild, *Prog. Polym. Sci.*, 1992, **17**, 163–249.

16 P. W. Barone and M. S. Strano, *Angew. Chem.*, 2006, **118**, 8318–8321.

17 (*a*) K. S. Novoselov, A. K. Geim, S. V. Morozov, D. Jiang, Y. Zhang, S. V. Dubonos, I. V. Grigorieva and A. A. Firsov, *Science*, 2004, **306**, 666–669; (*b*) A. K. Geim and K. S. Novoselov, *Nat. Mater.*, 2007, **6**, 183–191.

18 (*a*) Y. Wang, Z. H. Li, D. H. Hu, C. T. Lin, J. H. Li and Y. H. Lin, *J. Am. Chem. Soc.*, 2010, **132**, 9274–9276; (*b*) L. Feng and Z. Liu, *Nanomedicine*, 2011, **6**, 317–324.

19 (*a*) G. Eda, Y.-Y. Lin, C. Mattevi, H. Yamaguchi, H.-A. Chen, I. S. Chen, C.-W. Chen and M. Chhowalla, *Adv. Mater.*, 2010, **22**, 505–509; (*b*) C. H. Lu, H. H. Yang, C. L. Zhu, X. Chen and G. N. Chen, *Angew. Chem., Int. Ed.*, 2009, **48**, 4785–4787; (*c*) J. Kim, L. J. Cote, F. Kim and J. Huang, *J. Am. Chem. Soc.*, 2010, **132**, 260–267; (*d*) J. Balapanuru, J.-X. Yang, S. Xiao, Q. Bao, M. Jahan, L. Polavarapu, J. Wei, Q.-H. Xu and K. P. Loh, *Angew. Chem., Int. Ed.*, 2010, **49**, 6549–6553.

20 (*a*) Z. Liu, J. T. Robinson, X. M. Sun and H. J. Dai, *J. Am. Chem. Soc.*, 2008, **130**, 10876–10877; (*b*) J. T. Robinson, S. M. Tabakman, Y. Liang, H. Wang, H. Sanchez Casalongue, D. Vinh and H. Dai, *J. Am. Chem. Soc.*, 2011, **133**, 6825–6831.

21 W. S. Hummers and R. E. Offeman, *J. Am. Chem. Soc.*, 1958, **80**, 1339–1339.

22 (*a*) X. Sun, D. Luo, J. Liu and D. G. Evans, *ACS Nano*, 2010, **4**, 3381–3389; (*b*) S. Guo, S. Dong and E. Wang, *ACS Nano*, 2010, **4**, 547–555.

23 W. L. Wang, S. Meng and E. Kaxiras, *Nano Lett.*, 2008, **8**, 241–245.

24 (*a*) Y. Li, X. Fan, J. Qi, J. Ji, S. Wang, G. Zhang and F. Zhang, *Nano Res.*, 2010, **3**, 429–437; (*b*) J. Ji, G. Zhang, H. Chen, S. Wang, G. Zhang, F. Zhang and X. Fan, *Chem. Sci.*, 2011, **2**, 484–487; (*c*) D. R. Dreyer, H. P. Jia and C. W. Bielawski, *Angew. Chem., Int. Ed.*, 2010, **49**, 6813–6816; (*d*) G. M. Scheuermann, L. Rumi, P. Steurer, W. Bannwarth and R. Mulhaupt, *J. Am. Chem. Soc.*, 2009, **131**, 8262–8270.

25 (*a*) Y. Wei, S. Han, J. Kim, S. Soh and B. A. Grzybowski, *J. Am. Chem. Soc.*, 2010, **132**, 11018–11020; (*b*) N. K. Shrestha, J. M. Macak, F. Schmidt-Stein, R. Hahn, C. T. Mierke, B. Fabry and P. Schmuki, *Angew. Chem., Int. Ed.*, 2009, **48**, 969–972.

26 S. Underwood and P. Mulvaney, *Langmuir*, 1994, **10**, 3427–3430.

27 M.-Q. Zhu, L.-Q. Wang, G. J. Exarhos and A. D. Q. Li, *J. Am. Chem. Soc.*, 2004, **126**, 2656–2657.

28 R. Elghanian, J. J. Storhoff, R. C. Mucic, R. L. Letsinger and C. A. Mirkin, *Science*, 1997, **277**, 1078–1081.

29 J. T. Lai, D. Filla and R. Shea, *Macromolecules*, 2002, **35**, 6754–6756.

30 B. Nikoobakht and M. A. El-Sayed, *Chem. Mater.*, 2003, **15**, 1957–1962.

